RSC Advances

Bioavailability studies of curcumin-sophorolipid nano-conjugates in aqueous phase: Role in synthesis of uniform gold nanoparticles

Journal:	*RSC Advances*
Manuscript ID	RA-ART-05-2016-013469.R1
Article Type:	Paper
Date Submitted by the Author:	24-Jun-2016
Complete List of Authors:	Darne, Priti; National Chemical Laboratory, Biochemical sciences Mehta, Mihir; National Chemical Laboratory, Biochemical sciences Agawane, Sachin; National Chemical Laboratory, Biochemical sciences Prabhune, Asmita; National Chemical Laboratort, Biochemistry Division
Subject area & keyword:	Biomedical < Biological

Bioavailability studies of curcumin-sophorolipid nano-conjugates in aqueous phase: Role in synthesis of uniform gold nanoparticles

Priti A. Darne, ‡Mihir R. Mehta, ‡Sachin B. Agawane and Asmita A. Prabhune*

‡ Authors have contributed equally to the work.

Biochemical Sciences Division, CSIR- National Chemical Laboratory, Dr. Homi bhabha Road, Pune -411008, India. Email – aa.prabhune@ncl.res.in; Fax – 0202590 2648; Tel – 0202590 2239.

Abstract

The major limiting factors for curcumin to be accepted as a modern drug, despite its widespread applications are its lower aqueous solubility, less retention time and poor bioavailability. When subjected to a mild physical stress, curcumin is seen to internalize within the miceller hydrophobic core of Oleic Acid Sophorolipid resulting in the formation of Curcumin-Sophorolipid Nanoconjugates (CurSL). These bio-composite, shows enhanced retention time and increased bioavailability of curcumin in Rat models. In presence of gold salts, CurSL acts as a potent reducing and capping agents, resulting in the synthesis of monodispersed, spherical gold nanoparticles (CurSL-GNPs) of 8-10nm size. Physico-chemical, morphological and optical characteristics of both the nanoparticles are discussed based on spectroscopic absorption, photoluminescence (PL), dynamic light scattering (DLS), Zeta Potential, SEM and TEM measurements. FTIR spectroscopy signatures of these nanoparticles confirm the retention of functional groups in the end products. The retention time of 2 hours in blood plasma and increase in curcumin recovery by about 150 times than previously reported was observed in the pharmacokinetic (PKa) studies performed on Wistar rats. The bio-distribution of gold nanoparticles in rats was studied using EDX which showed their presence in different vital organs. Absence of unusual legions or necrosis in Histopathological analysis of vital organs in all the rat models suggests the use of curcumin-sophorolipid nano-conjugate for curcumin bioavailability and Cur-SL based nano-gold formulation as a good drug delivery carriers.

Key Words: Curcumin, Sophorolipid, Gold Nanoparticles, Retention time, HR-MS, SEM.

Introduction

Curcumin is the principle active ingredient of Turmeric, a popular ancient Indian spice, belonging to the *Zingiberaceae* (ginger) family and is responsible for the characteristic yellow color of turmeric[1]. Curcumin has extremely wide range of applications ranging from food and pharmaceutical industry to general well-being[2,3]. It is a polyphenolic compound consisting of two aromatic rings that provide hydrophobicity and tautomerism and influence the polarity of curcumin, while the linker olefin bond between the β-diketone provides flexibility[4-8]. Curcumin establishes its role in various activities like potent antioxidant, anti-proliferative, anti-inflammatory, anti-angiogenic, anti-metastatic, anti-diabetic, hepatoprotective, anti-atherosclerotic, anti-thrombotic, and anti-arthritic agent in cell culture, animal studies and clinical trials[9,10]. Studies also show curcumin to be potent against Cancer[11], Alzheimer's disease, Rheumatoid arthritis, hepatic disorders, cystic fibrosis, antineoplastic, anti-viral activity[1,4,5].

Reports of natural analogues of curcumin, curcuminoid derivatives and curcumin bio-conjugates have effectively been shown as anti-bacteria and anti-viral agent[12-14]. Researchers have also prepared solid dispersions of curcumin-polyvinyl pyrrolidone in a bid to increase its solubility and dissolution[15]. Curcumin nano crystals was proposed by Onoue et al in 2010 and Rachmawati et al. in 2012 using methods like milling and high pressure homogenization[16,17]. Polymer based nanoparticle formulation using poly (ε-Caprolactone)-poly (ethylene glycol)-poly (ε-Caprolactone) copolymer for self-assembly and delivery of curcumin in cancer is also reported[18]. Poly(lactic-co-glycolic acid) (PLGA) copolymer based Curcumin uptake was shown by Anand et al in 2010, Yallapu et al in 2010[19].

Despite these wide applicable properties, the hydrophobic nature of curcumin prevents the aqueous solubility resulting in negligible absorbance, easy elimination, excretion, no distribution, lower retention time and enhanced metabolism in the body which invariably restricts its use in pharma industry. All these factors combined together results in low plasma and tissue level concentration of curcumin which ultimately contributes towards curcumin being non bioavailable[11,12,14]. Various groups in the recent years have been positively working on improving the bioavailability of curcumin and explore its potential application as a modern drug.

An approach of micelles formation, which is an attractive and known property displayed by amphiphilic surfactants in hydrophilic or hydrophobic solutions (reverse micelles) is an emerging method used to address the solubility issue of hydrophobic drugs in water. Surfactants help in wetting of solids and hence improve the rate of disintegration of solids to smaller particles when applied with external physical force. Anisotropic water distribution in micelles aids in better entrapment of hydrophobic drugs within its core rather than adsorption on the surface of micelles. This also stabilizes the whole micelles-drug hybrid [20,21].

Hence to achieve the solubility of curcumin in water, we explore the use of non-ionic glycolipid surfactant viz. sophorolipid. Sophorolipids is a class of extracellular biosurfactants produced by a non-pathogenic yeast *Candida bombicola* (ATCC 22214). These molecules have a disaccharide unit (sophorose) linked by a glycosidic bond to the hydroxyl group at the penultimate carbon of monounsaturated C18 fatty acid. This arrangement of molecule renders sophorolipid its amphiphilic property[22]. Sophorolipids have negligible toxicity, higher biodegradability and the production media is derived from renewable sources. They are US FDA approved (oral route) for use in food and pharmaceutical industry[23].

To tackle the question of solubility of curcumin in water, we investigated the property of sophorolipids to form micelles while encapsulating curcumin to its core and forming nano-conjugates under physical force of sonication. The aspects of these nano-conjugates towards increase in bioavailability of curcumin in-vivo are studied in this manuscript. With complete characterization and animal studies, we compared the possibility of these conjugates as a next level or advances in the heavily researched area of drug solubility.

Also in the drug delivery facet, small and uniform metal nanoparticles are explored as safe carriers for drugs in-vivo. In this regards gold nanoparticles are vastly studied wherein gold salts are reduced generally by a reducing agent such as citric acid which leads to formation of gold nanoparticles. In addition, a stabilizing/capping agent is required in most cases and a surfactant plays this role efficiently either by adsorbing or chemically binding to the gold surface with the other end exposed in solution, thereby providing stability to the Au nanoparticles in colloidal solution and imparting charge on the particles which prevent aggregation and settlement [24].

The tunability and multivalent surface chemistry of Au nanoparticles elicit the potential to integrate multiple therapeutic molecules on the surface. And the stabilizing compound actually plays a very important role in toxicity of these particles *in vivo* [25]. Therefore, in this paper we have also ventured to study the gold nanoparticles synthesized using the curcumin-sophorolipid nanoconjugate in aqueous conditions. The characterization and the bio-distribution are examined in rat model which has been discussed here in detail

Materials and Methods

Reagents and Chemicals

All chemicals and reagents used in this study are of analytical grade unless mentioned otherwise. Curcumin 99%was procured from Sigma Aldrich, media components like peptone, yeast extract, malt extract were obtained from Hi-media, India and glucose from Qualigens, India. Sodium sulphate was purchased from Merck, India. Solvents namely Ethyl Acetate and Acetonitrile HPLC grade were procured from Rankem (India) and Merck, India respectively.

Organism and maintenance

Candida bombicola (ATCC 22214), a non-pathogenic yeast was maintained on MGYP slants at 4^{o}C which were subculture every four weeks prior to use for sophorolipid production. MGYP stands for Malt extract 0.3%, Glucose 2%, Yeast extract 0.3% and Peptone 0.5%[22].

Synthesis of oleic acid sophorolipid (OASL) and Extraction

Yeast *Candida bombicola* ATCC 22214 was used for the synthesis of Sophorolipid via resting cell method and Extraction, purification of sophorolipid is explained elsewhere[22].

Synthesis of aqueous Curcumin- Sophorolipid Nanoconjugates (CurSL)

The synthesis of sophorolipid induced curcumin nanoconjugates (CurSL) was initiated by adding 1mg of Curcumin and 40mg of OASL in 10mL distilled water. This suspension was then probe sonicated using Branson Digital Sonifier 250 at amplitude of 70 Hz with constant pulse of 10seconds at an interval of 3 seconds each for 40 minutes. The homogenous mixture thus obtained was a bright yellow colour dispersion of soluble curcumin in Sophorolipid solution.

Gold Nanoparticles synthesis

Gold nanoparticles (CurSL-GNPs) were synthesized using CurSL solution as a reducing and capping agent. Chloroauric acid ($HAuCl_4$) was added to 10ml of CurSL solution, making 1mM solution of $HAuCl_4$ and kept under 50^oC in water-bath at shaking condition of 50rpm for 1 hour.

Characterization

The UV-visible spectrum of the both dispersion CurSL and CurSL-GNP was recorded on a Jasco V-630 UV-Vis spectrophotometer. Spectrum from 200nm to 800nm was recorded using a 10 mm quartz cuvette cell. Curcumin (100µg/ml) dispersed in water was served as control for solubility in aqueous phase. Fluorescence spectroscopy was used to record the emission spectra for CurSL solution by providing excitation at 400nm on a Varian CARY 100 Bio UV-Vis spectrophotometer with a 10 mm quartz cell at 25 ± 0.1°C. Dynamic Light Scattering (DLS) using a "Brookhaven 90 plus nanoparticle size analyzer" instrument was employed to understand the hydrodynamic size of the particles in the dispersion and their zeta potential. The average surface charges of the particles were determined without diluting the prepared sample for both cases of CurSL solution and CurSL-GNPs. FTIR signatures of CurSL were studied on a Bruker, Alpha FTIR, over the spectral range of 450-4000 cm^{-1}.Controls used were curcumin (powder) and OASL individually. CurSL-GNPs FTIR signatures were also studied over the same range with 25 scans per sample. All FTIR signatures of the samples and controls were recorded in their nascent state.

Scanning Electron Microscopy (SEM)

The particles size and morphology of the dispersed particles of CurSL solution were obtained by visualizing them under SEM using a FEI Quanta 200 3D model. The dispersion was drop casted on a clean silicon wafer which was left to dry overnight. These were then sputtered with gold for enhanced contrast. The voltage provided was between 15-20 kV.

Transmission Electron Microscopy (TEM)

For CurSL-GNPs, 1:1 dilution of CurSL-GNP solution were drop casted on a carbon coated copper grid 200 mesh size obtained from Icon analyticals Pvt. Ltd, India and were left to dry over night. They were observed via TEM of FEI Technai G^2 200kV model.

Pharmacokinetic study

Nine Albino Wistar rats (approx. 200g) were the subject for this pharmacokinetic study. All the rats were housed under standard ethical conditions provided with *ad libitum* access to standard lab diet and water all throughout the experiment. The experiment on animals was conducted after obtaining permission from Institutional Animal Ethical Committee. The rats were divided into three groups; three each for curcumin control, CurSL nanoconjugates and CurSL-GNPs. All the animals were kept for fasting 12 hours prior to the start of the experiment. Three of the rats were orally administered with a dose of 1mL each of CurSL formulation containing 100µg of curcumin per 200 g body weight of each rats (maintaining 0.5mg/kg weight), while the control animals were provided with 100µg of standard curcumin dispersed in water. The CurSL-Gold Nanoparticles solution (1ml each) was administered as synthesized to the third group. The oral dosing was performed using a gavage of 3 inch long and 2.25mm diameter. Blood was collected alternatively (1mL) by retro-orbital method from venous plexus of rats at an interval of 0, 0.15, 0.30, 1, 2, 3, 4, 5, 6, and 24 hours into vials pre-treated with EDTA. The plasma from the blood samples were separated by centrifugation at 2000 rpm for 5 minutes at 10^{o}C. These plasma supernatant were collected and stored at -20^{o}C for further analysis.

HR-MS

The stored plasma specimens were thawed and precipitated in presence of acetonitrile[26]. The supernatant thus obtained was analyzed using HR-MS for the presence of curcumin traces. High resolution mass spectroscopy was performed on Thermo Scientific, Hybrid Quadrapole Q-Exactive orbitrap mass spectrometer to identify and analyze the presence of curcumin in the plasma samples. Liquid chromatography pump (Accela 1250) was used with Thermo Scientific Hypersil ODS C18 column 100 mm lengths with 3µm particle size. Isocratic solvent elution was carried out, using acetonitrile/water (60:40, v/v) with a flow rate of 0.5 mL/min for 15 minutes. The mass spectrometer was operated in positive electrospray ionization mode where the spray voltage was at 3.6kV, capillary temperature at 320°C, S-lens RF level at 50, automatic gain control (AGC) at 1×10^{6}, and maximum injection time at 120ms. Nitrogen was used as the sheath gas, sweep gas and auxiliary gas, set at 45, 10, and 2 (arbitrary units) respectively. A volume of 3 µL of sample was injected and full HR-MS scan was performed using positive polarity. Data was analyzed with Thermo Scientific Xcalibur software. The mass spectra associated with chromatographic peaks were analyzed for

Curcumin control, CurSL solution administered in rat and compared with Curcumin standard in acetonitrile.

Histopathological study

After 48 hours of administration of CurSL formulation, rats were sacrificed and part of their lung, spleen, liver, heart, and kidney were fixed in 10% formalin for preparation of histopathological slides. The tissues were processed in a Leica TP 1020 tissue processor, and then embedded in paraffin blocks using Leica EG 1160 paraffin embedder. The paraffin blocks were cut into ribbons of 4 mm using a Microm HM 360 microtome. The slides were stained in hemotoxylin and eosin using a Microm HMS-70 stainer. The permanent slides were made and evaluated for histopathological changes under Olympus BX51 microscope, this study was carried out to test the toxicity of formulation on organs of the administered rats.

The same organs were collected from rats administered with CurSL-GNPs and these organs were lyophilized to obtain powder. EDX analysis was carried out on SEM instrument of FEI Quanta 200 3D model to analyse the distribution of gold nanoparticles in rat.

Results and Discussion

Spectrophotometric analysis

After the synthesis of Curcumin-sophorolipid Nanoconjugates (CurSL), a UV-visible spectrum of the solution was recorded to understand their solubility in aqueous solution. Fig 1a; represents the UV-Vis spectra of CurSL in aqueous solution in comparison with curcumin dispersed in water. The spectrum showed a peak at 424nm whereas; the lambda maximum of curcumin in water was at 440nm with relatively very less absorbance. Curcumin in any medium is very sensitive regarding its photo-physical properties and shows strong absorbance at varying wavelengths[27]. The soluble curcumin usually absorbs at 420nm in organic solvents[28]. In our case we observed that CurSL nano-conjugate showed perfect peak at 424nm which points to curcumin being soluble in the sophorolipid solution. But same was not observed for curcumn in water. This might be due to insoluble nature of curcumin in water where the fine particles in dispersion are seen to absorb at 440nm when taken a UV-Vis spectrometry of solution. OASL in solution did not show any significant absorbance which can be easily seen in the Fig 1a.

The physical stress (sonication) that the sophorolipids are subjected to, as mentioned in our methods causes them to form spherical micelles making them suitable vessels for drug delivery [29]. Sophorolipids are known to form micellelar assemblies from concentration of 5mg/ml to 50mg/ml[30]. Here the sophorolipids micelles internalize curcumin in the hydrophobic core, whereas the hydrophilic component of the sophorolipids remains on the outer surface exposed to interact freely with the aqueous environment enabling curcumin solubility[28].

Furthermore CurSL solution was used as reducing and capping agent for the formation of gold nanoparticles at 50^{o}C temperature. Chloroauric acid (1mM) got converted into gold nanoparticles giving characteristic purple colored solution within one hour. This is very well evident from the UV spectrum having λ_{max} at 540nm which is typical of gold nanoparticles [31] shown in Fig.1b. A sharp SPR band was observed which implies that the aggregation of the nanoparticles is very slow and the solution is relatively stable[32]. Generally, the difference in the intensity of SPR bands is attributed to diverse levels of size distribution of particles as well as their shape in the solution along with their aggregation[33, 34].

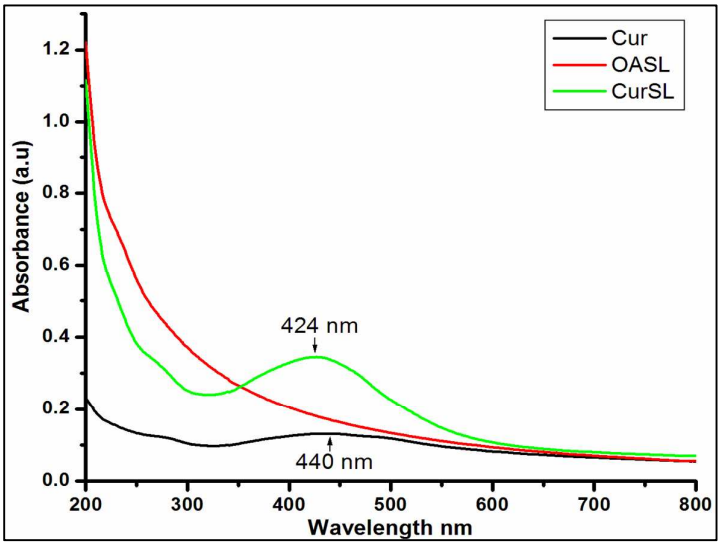

Fig.1a. The UV-Vis spectrum of Curcumin in water, sophorolipid (OASL) solution and synthesized CurSL nano-conjugate solution. λmax observed at 424nm and 440nm for CurSL and Curcumin in water respectively.

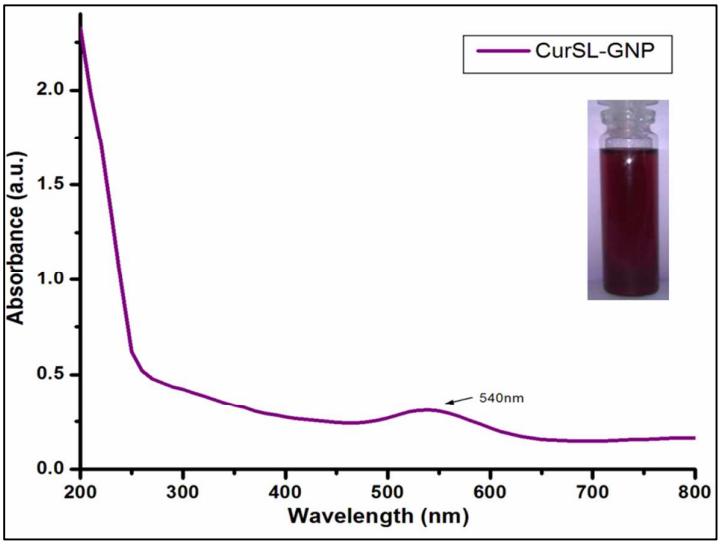

Fig.1b. The UV-Vis spectra of CurSL-GNPs, where λmax is observed at 540nm.

The Photoluminescence (PL) data of Oleic Acid sophorolipid (SL), Curcumin (Cur) in water and the synthesized Curcumin-Sophorolipid nano-cojugate (CurSL) solution showed a considerable blue shift. This is of about 50nm in reference to curcumin control similar to that of the UV-Vis spectra [28]. The PL was recorded at the excitation of 400nm in aqueous solution for all three samples giving us the best comparative results. SL exhibited no photoluminescence, whereas curcumin in aqueous solution displayed a week excitonic emission at 548nm because of its poor aqueous solubility. However CurSL nano-conjugate on excitation at wavelength of 400nm exhibited a manifold rise in its intensity yielding a strong emission at 504nm which concretes the results of strong green fluorescence. In accordance with this observation, a bright yellow colored dispersion of evenly distributed curcumin nano-conjugates is seen in Fig. 2 which emits sharp green fluorescence under UV light.

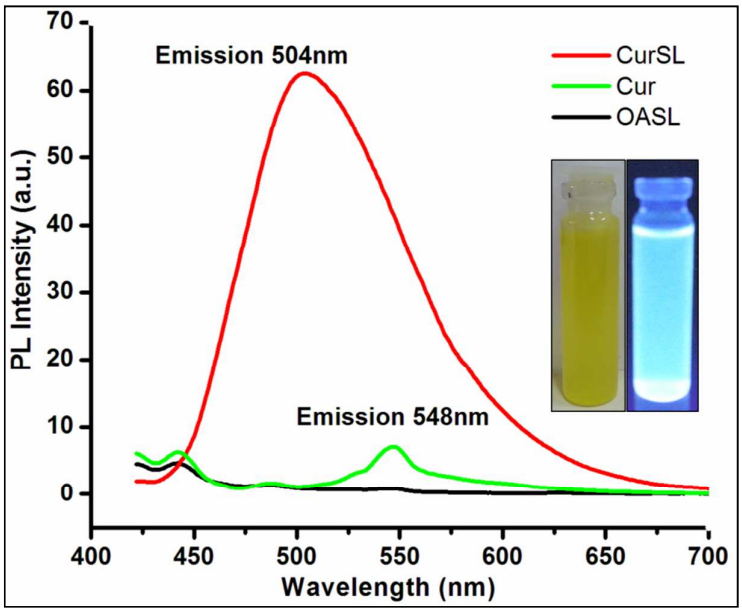

Fig.2. The PL spectra when excited at 400nm for CurSL nano-conjugate, curcumin (cur) in water and sophorolipid (OASL) solution. Emission λmax was observed at 504nm and 548nm with the inset images of solutions for CurSL nano-conjugate and curcumin (cur) in water respectively.

FTIR Characterization

FTIR spectroscopy was performed to contemplate the chemical changes in curcumin, OASL, CurSL conjugate and CurSL-GNPs that may have occurred during the synthesis process. The curcumin (powder) spectrum showed all the relevant bands including the characteristic 1556cm^{-1} of the C-C aromatic group, 1628cm^{-1} and 1717cm^{-1} of C=O (keto) stretch and 1412cm^{-1} of C-O (enol) stretch. On the other hand, sophorolipid spectrum displayed a C-H alkane bend at1380cm^{-1} and an aliphatic stretch at 2909cm^{-1} and 2980 cm^{-1}.

While in the spectra of CurSL solution all the bands of the parent molecules were observed, apart from the signature band representing the enol bending of curcumin. In this conjugate, the enol group may be subdued due to the presences of SL micelles. Additionally the CurSL conjugate showed presence of a C-O-H duplet at 1226cm^{-1}. This additional group may be formed as a result of the interaction between the enol group of curcumin and SL in the solution causing a minor shift in the keto group.

The CurSL-GNPs on the other hand had very less observable bands viz. 719cm^{-1}, 1753cm^{-1} and 3319cm^{-1} indicating the presence of C-H bend,C=O stretch of Keto and phenolic OH

stretch respectively. As the GNPs are stabilized, there was a prominent shift in the keto group from 1628cm^{-1} to 1753cm^{-1}with respect to that of curcumin. This shift is due to the loss of the hydrogen present in the subdued enolic group, in presence of a strong oxidizing $AuCl_4$ salt[35]. Table 1 mentions the wavelengths and their representing bonds. All these values are consenting with the literature surveyed [28, 36-42].

Table 1: FTIR signatures and their representing bonds

Cur	**CurSL**	**OASL**	**CurSL-GNP**	**Bonds**
717, 886, 976	714	783, 896	719	C-H bend
1014, 1119, 1179	1187	1125, 1179		C-O stretch
	1226			C -O-H bend
1301	1314	1313		C-O stretch
	1391	1380		C-H alkane bend
1412				C-O enol bending
1556	1509, 1581	1503, 1574		C-C aromatic
1628, 1717	1759		1753	C=O stretch of Keto
	1840	1840		Acid anhydride
	2911, 2979	2909, 2980		Alkane stretch
3526	3310, 3364	3410	3319	OH phenolic stretch

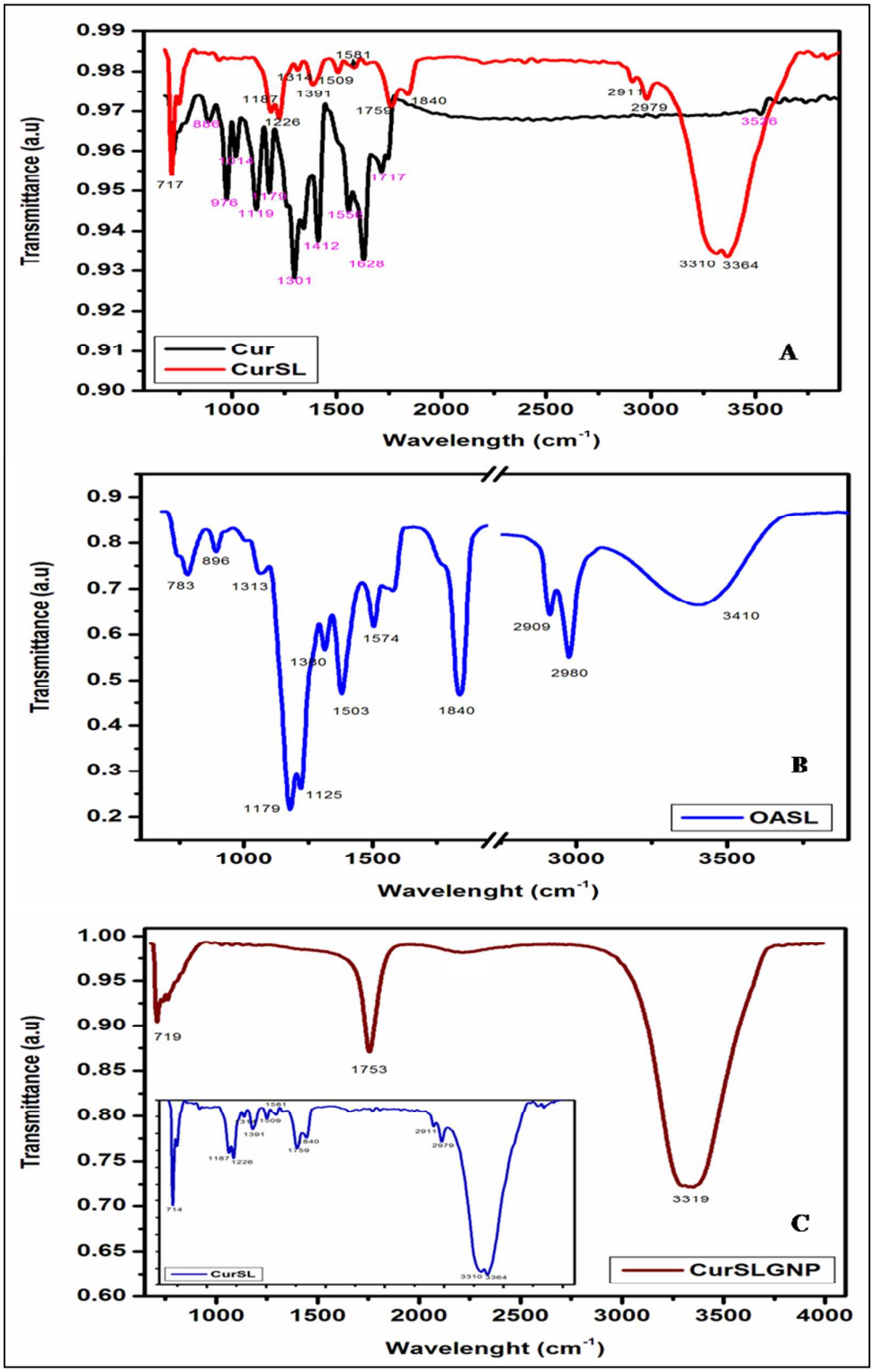

Fig. 3: FTIR analysis of (A) Curcumin (powder) and CurSL solution, (B) OASL and (C) CurSL-GNP, inset CurSL solution.

Particle Size Distribution and Stability

The particle size of the CurSL nano-conjugates in aqueous solution was measured using the DLS spectra (Fig. 4a.) revealed the formation of monodispersed nanoparticles. The average hydrodynamic size as calculated was around 275nm with a mean polydispersity index of 0.2. The morphology and particle size distribution using SEM images (Fig. 5b.) of nanoparticles correlates with the DLS analysis. SEM was performed on curcumin dispersed in water as curcumin control (Fig. 5a.). SEM images confirmed that the irregular shaped curcumin was converted into nearly spherical shaped nanoparticles in presence of sophorolipids with an average size of 40-60nm. This extreme size reduction and monodispersity was achieved as a result of physical impulse imparted due to probe sonication in presence of the amphiphilic, biosurfactant SL. Moreover, the surfactant facilitates in reducing the interfacial surface tension enabling synthesis of evenly dispersed nearly spherical nanoparticles[28]. CurSL-GNPs were also subjected for DLS analysis (Fig. 4c.), where it was observed that the polydispersity of these particles is 0.3 and the hydrodynamic size was found to be 5nm. The TEM analysis (Fig. 5c.) confirms the size of gold nanoparticles to be nearly 5-10nm which is in agreement with DLS.

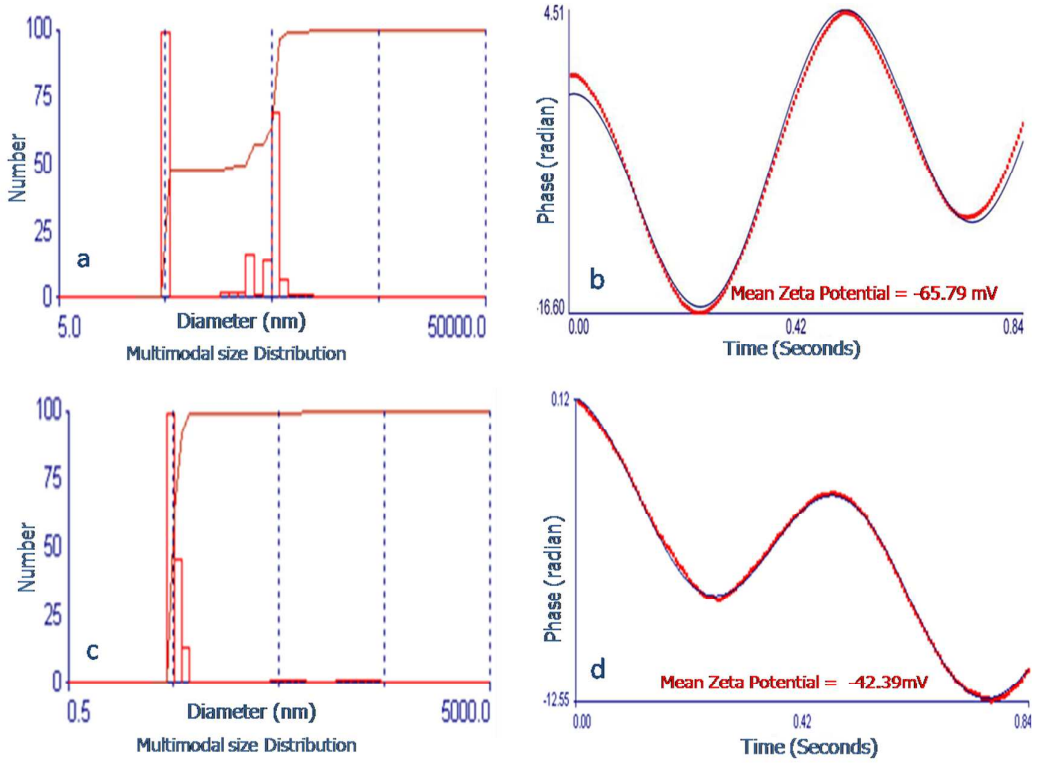

Fig. 4: (a) DLS and **(b)** Zeta Potential of synthesized CurSL nanoparticles indicating the hydrodynamic size of 275nm and the mean zeta potential of -65.79 mV.**(c)** DLS of CurSL-GNPs with hydrodynamic size as 5nm and -42.39 mV zeta potential **(d)**.

Zeta Potential was measured to understand the surface charge and electric potential of CurSL nano-conjugates which is complementary to its stability in aqueous solution [43]. The stability of the solution is in agreement with the calculated zeta potential which shows that the mean surface charge of CurSL nano-conjugates is -65.79mV (Fig. 4b.) which is considered extremely stable[32,42]. K. Sindhu et al, 2013 used green approach to synthesize gold nanoparticles using curcumin alone by manipulating pH to attain spherical shape, and stability upto 6 months with -23mV zeta potential[44], but the synthesis given in this paper is able to get Gold nanoparticles with higher stablility having a zeta potential of -42.39mV (Fig. 4d.). The size of these CurSL-GNPs was observed to be 5-10nm via TEM and DLS. The properties and stability of Cur-SL-GNP solution were retained even after a year.

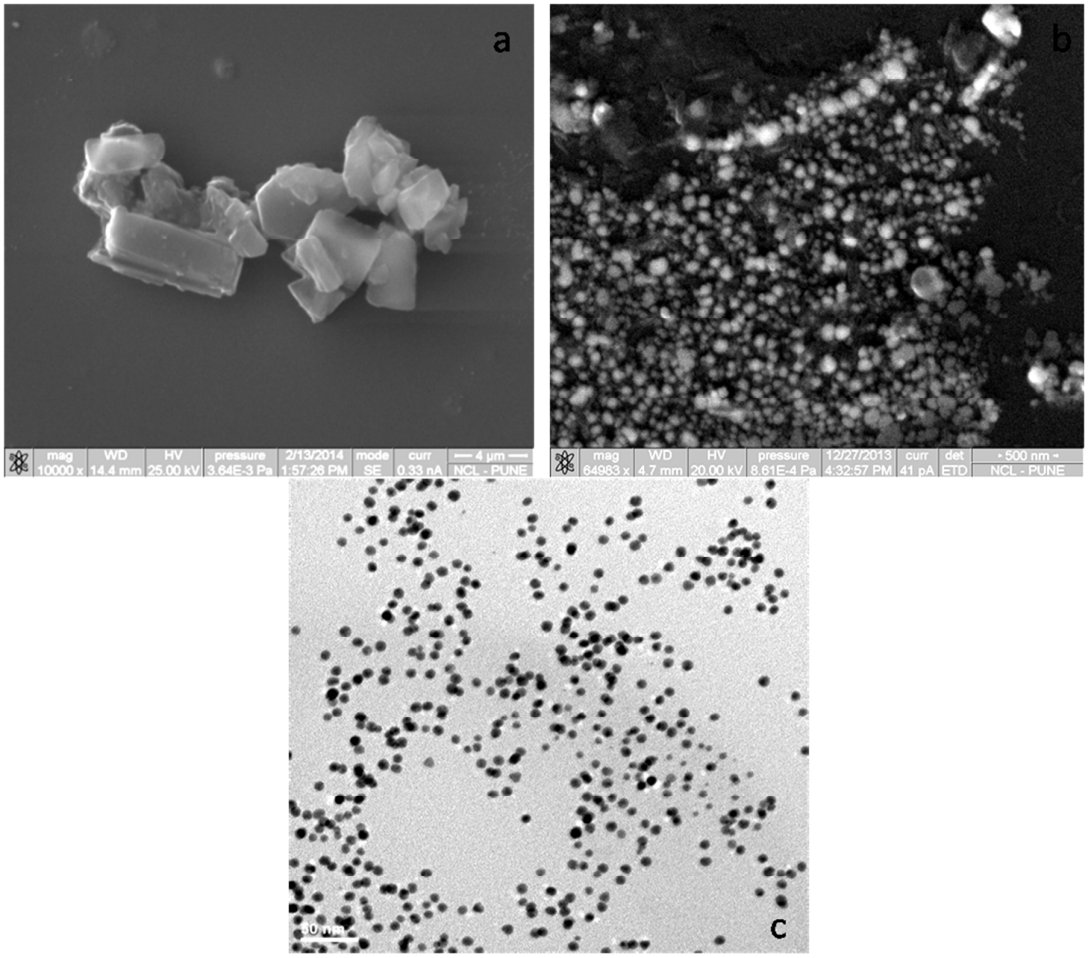

Fig.5: SEM images of Curcumin control **(a)** showing large irregular pieces about 8-10μ in size. **(b)** CurSL solution evenly dispersed nearly spherical nanoparticles of size between 40-60nm. **(c)** TEM image of CurSL-GNPs, scale represented is 50nm and the size of particles is nearly 8-10nm.

Pharmacokinetic Plasma Studies:

The pharmacokinetics of curcumin has been ambiguously explained due to its extremely poor water solubility, poor bioavailability and rapid degradation within the body[45]. This leads to indistinguishable level of curcumin in the plasma, making the calculations of pharmacokinetic very difficult to study. It has also been reported in many studies about the intrinsic properties of curcumin and its ability to act as a therapeutic agent for a host of ailments[12]. Nonetheless most of these reports lament about poor oral and intestinal bioavailability (≈11ng/ml) to be one of the biggest barriers for curcumin to exhibit the wide range of its medicinal properties[46]. It has also been studied that even after administration of about 12g/ml of curcumin through oral route to human, negligible amount of 50ng/ml was recovered from the serum[47].

In one of the studies reported by Ravindranath et al 1980, showed that only trace amounts of curcumin, as low as 5μg/ml was found in the blood portal of Rats even when 400mg of curcumin was administered[48]. In another time-bound experiment, when a single dose of 2g/kg of curcumin was administered to rats, maximum quantity of 1.35μg/ml was recovered from the serum sample after 0.83 hours whereas in human after 1 hour as low as 0.006μg/ml was recovered[12].

Pan et al 1998 explored the pharmacokinetic properties of curcumin in mice, by oral administration. They found that after oral administration of 1g/kg of curcumin, the maximum amount found in their plasma was a mere 0.22μg/ml which was obtained after 1 hour; the plasma concentration was further declined with increase in time[49]. According to a recent study conducted by Anand P et al., 2007[12], distinct peak of curcumin was seen after an hour in the serum sample of curcumin treated to nude mice. After administering 1 g curcumin per kg rats through the oral route, the maximum serum curcumin level noted was as low as 0.5μg/mL after 45 minutes of dosing[50]. Furthermore, a few other studies displayed maximum retention of 6.5 ± 4.5 nM of curcumin after 0.5 hours[51] in male rats.

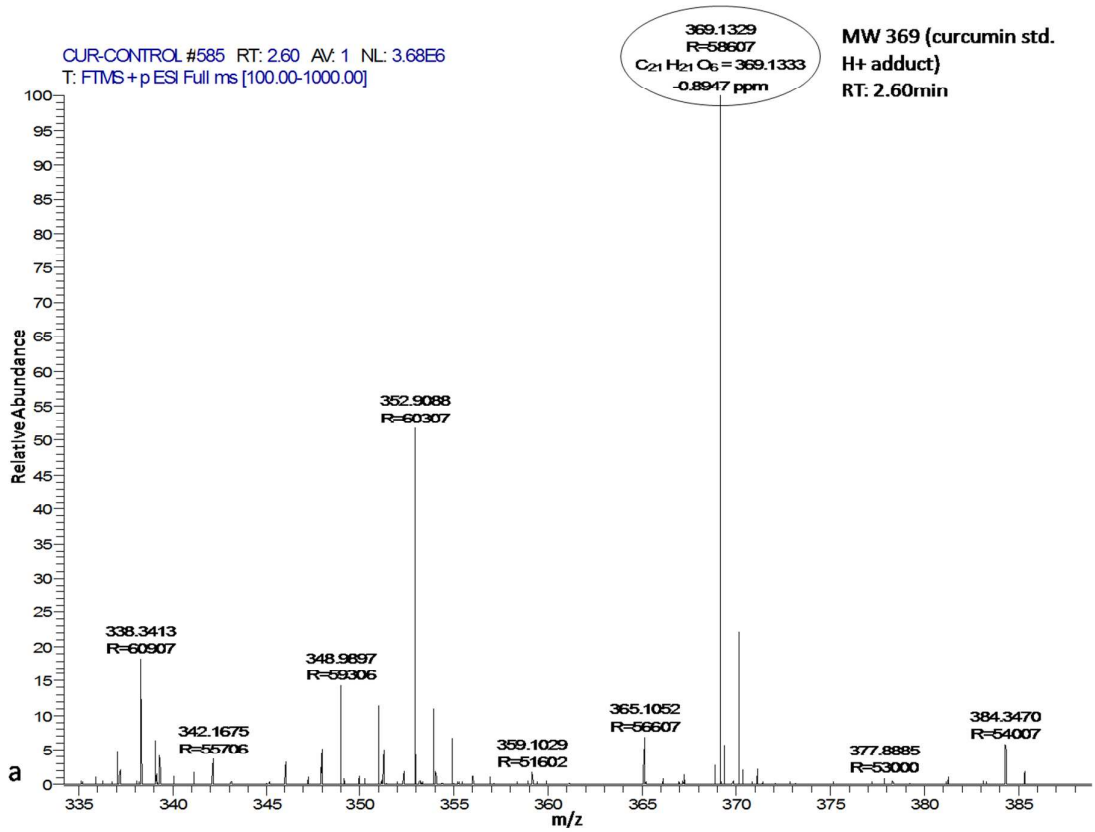
CUR-CONTROL #585 RT: 2.60 AV: 1 NL: 3.68E6
T: FTMS + p ESI Full ms [100.00-1000.00]
369.1329
R=58607
C21 H21 O6 = 369.1333
-0.8947 ppm
MW 369 (curcumin std.
H+ adduct)
RT: 2.60min
352.9088
R=60307
338.3413
R=60907
348.9897
R=59306
342.1675
R=55706
359.1029
R=51602
365.1052
R=56607
377.8885
R=53000
384.3470
R=54007
Relative Abundance
m/z
a

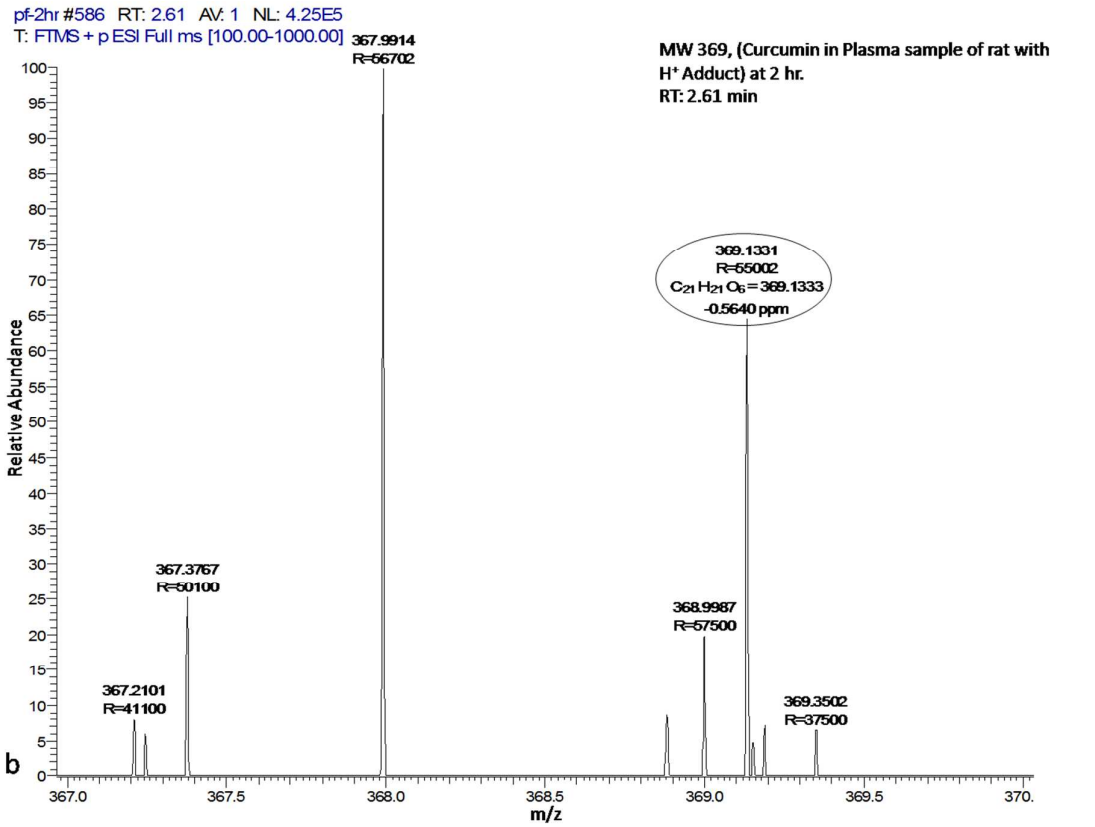
pf-2hr #586 RT: 2.61 AV: 1 NL: 4.25E5
T: FTMS + p ESI Full ms [100.00-1000.00]
367.9914
R=56702
MW 369, (Curcumin in Plasma sample of rat with
H+ Adduct) at 2 hr.
RT: 2.61 min
369.1331
R=65002
C21 H21 O6 = 369.1333
-0.5640 ppm
367.3767
R=60100
368.9987
R=57500
367.2101
R=41100
369.3502
R=37500
Relative Abundance
m/z
b

Fig. 6: An HR-MS spectrum of standard curcumin in ACN (a)and spectrum of extracted plasma samples from Wistar rats administered with CurSL (100µg/ml) solution after 2 hr time interval (b).

In our present investigation, as described in the experimental section 100µg of curcumin in the form of CurSL was administered orally per ~200g of rats. The retention time and bioavailability of CurSL was compared with that of standard curcumin in water administered in rats. Standard sample was prepared by dissolving curcumin in acetonitrile (ACN) and a method was developed on the HPLC for which an isocratic system of ACN: Water (60:40) at 424nm was set for 15 minutes. Same parameters were assigned on the HR-MS instrument for which a single sharp peak was observed at a retention time of 2.61 minutes as seen in Fig. 6a. and 6b. Plasma samples from both the groups of rats (Control and CurSL treated) were collected at various time intervals and treated with ACN to denature the proteins and other plasma components[52-54]. Following this, the plasma samples were eluted employing the above mentioned method by HR-MS technique. The chromatogram of HR-MS in supplementary data for the plasma samples collected at all the time intervals of the control animals showed no elution of curcumin at the retention time of 2.61 minutes. On the other hand, plasma samples of the rats administered with CurSL solution display a prominent peak at the same elution time (2.61 min) as that of the standard at the end of two hours. As there was no further elution of curcumin in the following time intervals, it can be vividly said that CurSL solution was retained in the animals for at least two hours. From this study, we illustrated that intact curcumin was made bioavailable with enhanced retention of up to two hours when 100µg of curcumin (CurSL) was orally delivered to ~200g of rats.

For calculating the exact amount of curcumin found in the plasma of CurSL solution treated rats, a standard Curcumin of 1µg/ml in Acetonitrile was subjected to HR-MS analysis using same column and conditions that were provided for animal study sample (Supplementary information). From the results of the plasma studies (Fig. 6b.), the Normalized Level (NL) of curcumin after two hours, was noted to be 4.25×10^5 and that of standard Curcumin (1µg /ml) was marked to be 2.68×10^7. Calculations based on these values showed the concentration of curcumin present in the collected plasma sample after two hours to be nearly 15.87ng/ml of blood. The overall percentage of curcumin in plasma was calculated to be 0.015%. This percentage is many folds higher than that of Pan et al 1998 [49] and Maiti et al 2007 [50] which could achieve 0.00011% and 0.00025% respectively (supplementary data) when administered with 1g/kg of curcumin to rats.

Histopathological Analysis

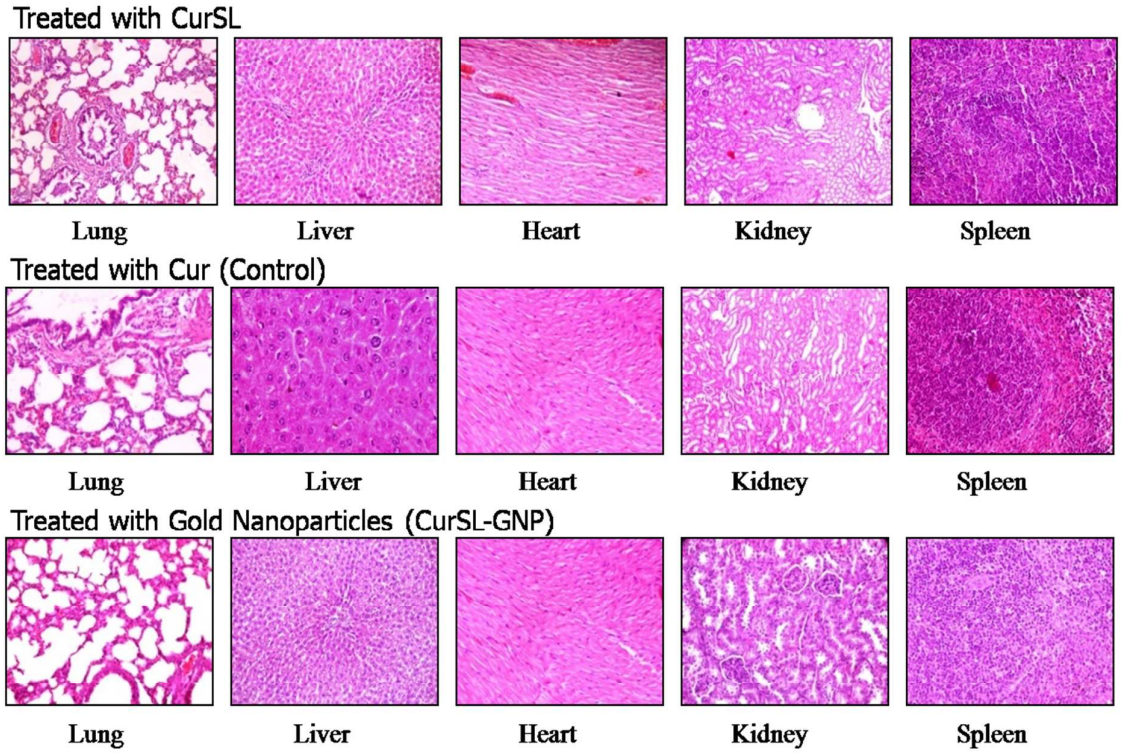

Fig.7: Microscopic images of the Histopathology of organs viz., Lung, Liver, Heart, Kidney and Spleen.

Once the blood collection for plasma analysis was completed at 48hours, the animals were sacrificed by cervical dislocation. The vital organs of rats from each group viz. CurSL, curcumin control and CurSL-GNP were instantly fixed in 10% formalin solution. As described in the methodology above, slides of organs were made and analyzed under light microscope to study any abnormal changes in their cell structure. It was observed that all the animal organs were completely normal with no unusual legions or necrosis. From this it can be concluded that the CurSL solution and CurSL-GNPs are safe to deliver *in vivo*.

EDX analysis

Part of the vital organs of rats that were administered with CurSL-GNPs were kept in -20^{o}C immediately after their removal from rat body. They were then transferred to -80^{o}C deep freezer for 3-4hours. Later these organs were lyophilized to remove all the moisture from them and then they were ground to fine powder. This powder was subjected to Energy Dispersive X-Ray (EDX) analysis provided by SEM using a FEI Quanta 200 3D model.

Table 2 indicates the Carbon and Oxygen Weight % element along with the Au from organs viz. Heart, Kidney, Lung, Liver and Spleen.

Table 2: Weight % by Element from EDX analysis

Organs	CK	OK	AuL
Heart	38.04	22.28	2.78
Kidney	36.17	37.88	3.11
Lung	37.42	31.97	5.59
Liver	39.36	35.02	1.74
Spleen	35.98	39.69	2.38

In our previous studies we have reported use of sophorolipid for synergistic delivery and activity of antibiotic. It was theorized that SL spans the cell membrane and delivers the drug within the cell[23]. Also sophorolipid were used to cap CdTe quantum dots (QDs) to understand the compatibility of QDs on normal and cancer cell line using MTT assay for Theranostic application. It was observed that SL- capped CdTe particles showed biocompatibility with both the cell lines and enhanced the cellular association and uptake of QDs[55]. From these results we can hypothesize that, Sophorolipid being amphiphilic in nature may cross the cell membrane and assist the CurSL-GNPs obtained in this report (range of 8-10nm which is nearly quantum dots size) as drug carrier which can cross the Blood Brain Barrier (BBB).

Conclusion:

There is extensive ongoing research among various groups to solubilize curcumin in aqueous solution and improve its bioavailability. One of the aspects for curcumin solubilization is to maintain its properties without altering its structure and chemical bonds. Keeping these concerns in mind, we have solubilized curcumin in miceller aqueous solution of sophorolipids resulting in the synthesis of curcumin nanoconjugates. Employing the physical force of sonication, we were able to form CurSL nanoconjugates of size in the range of 40-60nm confirmed by SEM and DLS. The physico-chemical characterization of CurSL displayed a significant blue shift for maximum absorbance when measured on a UV-Visible spectroscopy with respect to the non-solubilized curcumin in water. PL studies showed a bright green fluorescence emitted by CurSL sample at 504nm when excited at 400nm. During their synthesis, significant chemical bonds were retained indicating no chemical modifications with respect to standard curcumin as indicated by FTIR signatures. This data is

of great significance as any structural and chemical changes in curcumin can result in loss or modification of activity. The synthesis of CurSL-GNPs was also achieved at ambient temperatures unlike that of the earlier reported studies by Singh et al 2013, where they have used 90^{o}C temperature which may lead to loss in activity of curcumin. The rate determining step for oral drug formulation is absorption by the gastrointestinal tract with respect to the dissolution and solubility in aqueous solution[20]. The synthesized CurSL nanoparticles when administered to Wistar rats for bioavailability study, showed remarkable increase in retention time of curcumin in blood plasma up to 2hours.The concentration of curcumin in blood plasma was 0.015% which was calculated using HR-MS data of standard curcumin of 1µg/ml and which is much higher than 0.00011%[49] and 0.00025%[50] of previous reports. The bio-distribution of CurSL-GNPs in rat showed presence in all vital organs. The uniform, nanosize of gold nanoparticles can be further tagged with hydrophobic drugs for delivery and slow release of drugs which may even carry them and cross BBB. Our method of solubilization of curcumin can become a solution for the use of curcumin as therapeutic drug in modern science.

Acknowledgement

Authors would like to thank CSIR for providing with funds under the 12th5 year plan project Advanced Drug Delivery Systems (CSC0302). Also authors are thankful to Center for Material Characterization division of NCL for providing with world class instruments for characterization studies and Symbiosis School of Biomedical Sciences for permission to carry animal studies in their premises.

References

1) M. Akram, S. A. Ahmed, K. Usmanghani, A. Hannan, E. Mohiuddin, and M. Asif, *Rom. J. Biol. Plant Biol,* 2010, 55 (2), 65–70.
2) Y. Wang, Z. Lu, F. Lv and X. Bie, *Eur Food Res Technol* , 2009, 229, 391–396
3) O. Naksuriya, S. Okonogi, R. M. Schiffelers and W. E. Hennink, *Biomaterials,* 2014, 35, 3365-3383
4) H. Hatcher, R. Planalp, J. Cho, F. M. Torti and S. V. Torti, *Cell. Mol. Life Sci*., 2008, 65, 1631 – 1652.
5) S. Balasubramanian, A. R. Girija, Y. Nagaoka, S. Iwai, M. Suzuki, V. Kizhikkilot, Y. Yoshida, T. Maekawa, and S. D. Nair, *International Journal of Nanomedicine*, 2014, 9,437–459.

6) R.A. Sharma, A.J. Gescher, W.P. Steward. *European Journal of Cancer*, 2005, 41, 1955–1968.

7) K. S. Bhullar, A. Jha, D. Youssef and H. P. V. Rupasinghe, *Molecules,* 2013, *18*, 5389-5404.

8) S. C. Gupta, S. Prasad, J. H. Kim, S. Patchva, L. J. Webb, I. K. Priyadarsini and B. B. Aggarwal, *Nat. Prod. Rep.*, 2011, 28, 1937–1955.

9) S. C. Gupta, S. Patchva, and B. B. Aggarwal, *AAPS Journal*, 2013, 15(1), 195-218.

10) S. S. Bansal, M. Goel, F. Aqil, M. V. Vadhanam, and R. C. Gupta, *Cancer Prev Res (Phila)*, 2011, 4(8), 1158–1171.

11) R. Jäger, R. P. Lowery, A. V. Calvanese, J. M Joy, M. Purpura and J. M. Wilson, *Nutrition Journal*, 2014, 13, 11.

12) P. Anand, A.B. Kunnumakkara, R. A. Newman and Bharat B. Aggarwal, *Mol. Pharmaceutics*, 2007, 4 (6), 807-818.

13) M.K. Kim, H. Mok and Y. Chong, *Bull. Korean Chem. Soc.*, 2012, 33 (9), 2849.

14) R.K. Singh, D. Rai, D. Yadav, A. Bhargava, J. Balzarini and E. De. Clercq, *European Journal of Medicinal Chemistry*, 2010, 45, 1078–1086.

15) N. Kaewnopparat, S. Kaewnopparat, A. Jangwang, D. Maneenaun, T. Chuchome and P. Panichayupakaranant, *World Academy of Science, Engineering and Technology*, 2009, 3, 7-29.

16) S. Onoue, H. Takahashi, Y. Kawabata, Y. Seto, J. Hatanaka, B. Timmermann, S. Yamada, *J Pharm Sci.*, 2010, 99 (4), 1871-81.

17) H. Rachmawati, L. Al Shaal, R. H. Müller, C. M. Keck, *Journal of Pharmaceutical Sciences*, 2013, 102(1), 204-214.

18) R. Feng, Z. Song, G. Zhai, *International Journal of Nanomedicine,* 2012, 7, 4089–4098.

19) H. Rachmawati, *Int. J. Res. Pharm. Sci.*, 2013, 4(2), 211-220.

20) K.T.Savjani, A.K. Gajjar and J.K. Savjani, *International Scholarly Research Network*, 2012, 10.

21) S. Gokturk, E.Caliskan, R. Y. Talman and U. Var, *The Scientific World Journal*, 2012, 12

22) P. Darne, M. Mehta, P. Dubey and A. Prabhune, *World Journal of Pharmacy and Pharmaceutical Sciences*, 2014, 3 (11), 792-804.

23) K. Joshi-Navare and A. Prabhune, *BioMed Research International,* 2013, 10.1155.

24) R. A. Sperling, P. R. Gil, F. Zhang, M. Zanella and W. J. Parak, *Chem. Soc. Rev.*, 2008, 37, 1896–1908.

25) D. A. Giljohann, D. S. Seferos, W. L. Daniel, M. D. Massich, P. C. Patel, and C. A. Mirkin, *Angew Chem. Int. Ed.,* 2010, 49, 3280 – 3294.

26) L. Zhongfa, M. Chiu, J. Wang, W. Chen, W. Yen, P. Fan-Havard, L. D. Yee and K. K. Chan, *Cancer ChemotherPharmacol.* 2012, 69 (3), 679–689.

27) A. Barik, K.I. Priyadarsini and H. Mohan, *Photochemistry and photobiology*, 2003, 77(6), 597-603.

28) P. K. Singh, K. Wani, R. Kaul-Ghanekar, A. Prabhune and S. Ogale, *RSC Adv.*, 2014, 4, 60334-41.

29) P. Dubey, K. Selvaraj and A. Prabhune, *World Journal of Pharmacy and Pharmaceutical Sciences*, 2013, 2 (3), 1107-1133.

30) N. Baccile, F. Babonneau, J. Jestin, G. Pehau-Arnaudet, and I. Van Bogaert, ACS Nano, 2012, 6 (6), 4763–4776.

31) A. Rai, A. Prabhune and C. C. Perry, *J. Mater. Chem.*, 2010, 20, 6789–6798.

32) R. Jagannathan, P.M. Abraham and P. Poddar, *J. Phys. Chem. B,* 2012, 116, 14533-14540.

33) D.K. Singh, R. Jagannathan, P. Khandelwal, P. M. Abraham and P. Poddar, *Nanoscale*, 2013, 5, 1882.

34) W. Rechberger, A. Hohenau, A. Leitner, J.K Krenn, B.Lamprecht and F.R. Aussenegg, *Optics communications 220*, 2003, 137-141.

35) C. Sreelakshmi, N. Goel, K.K.R. Datta, A. Addlagatta, R. Ummanni, and B. V. Subba Reddy, *Nanosci. Nanotechnol. Lett.*, 5, 2013, 1–8.

36) Typical Infrared Absorption Frequencies, http://staff.aub.edu.lb/~tg02/IR.pdf, (accessed December 2015).

37) Infrared Spectroscopy, http://www.biomaterial.com.br/FTIR.pdf, (accessed December 2015).

38) S. Bakkialakshmi and G. Jayaranjani, *IJPCBS*, 2015, 5(1), 93-97.

39) S. S. Solanki, P. Paliwal, S. Jain, P. Sharma, and B. Sarkar, *Current Research in Pharmaceutical Sciences*, 2012, 04, 210-214,

40) S. F. Chow, L. Shi, W. Wing Ng, K. H. Yan Leung, K. Nagapudi, C. C. Sun and A. H. L. Chow, *Cryst. Growth Des.,* 2014, 14, 5079−5089.

41) S. N. Abd El-Rahman and S. S. Al-Jameel, *Sch. Acad. J. Biosci.*, 2014, 2(3), 214-223.

42) M. Ibrahim, M. Alaam, H. El-Haes, A.F. Jalbout and A. Leon, *Ecletica Quimica,* 2006, 31, 3.

43) C. Moorthi, K. Krishnan, R. Manavalan and K. Kathiresan, *Asian Pac J Trop Biomed*, 2012, 2(11), 841-848.

44) K. Sindhu, A. Rajaram, K. J. Sreeram and Rama Rajaram, *RSC Adv.*, 2014, 4, 1808-1818.

45) Y. B. Pawar, B. Munjal, S. Arora, M. Karwa, G. Kohli, J.K. Paliwal and A.K. Bansal, *Pharmaceutics*, 2012, 4, 517-530.

46) M.H. Ucisik, S. Kupcu, B. Schuster and U. B. Sleytr, *Journal of Nanobiotechnology*, 2013, 11, 37.

47) C.D. Lao, M.T. Ruffin IV, D. Normolle, D. D. Heath, S. I. Murray, J. M. Bailey, M. E. Boggs, J. Crowell, C. L. Rock and D. E. Brenner, *BMC Complementary and Alternative Medicine*, 2006, 6, 10.

48) V. Ravindranath and N. Chandrashekhara, *Toxicology*, 1980, 16(3), 259-265.

49) M. Pan, T. Huang and J. Lin, *Drug Metabolism and Disposition*, 1998, 27(1), 486-494.

50) K. Maiti, K. Mukhurjee, A. Gantait, B. P. Saha and P.K. Mukhurjee, *International Journal of Pharmaceutics*, 2007, 330(1-2), 155-163.

51) T. H. Marczylo, R.D. Verschoyle, D.N. Cooke, P. Morazzoni, W.P. Steward and A. J. Gescher, *Cancer Chemotherapy and Pharmacology*, 2007, 60 (2), 171-177.

52) S. D. Garbis, A. Melse-Boonstra, C.E. West and R.B. van Breemen, *Anal. Chem.*, 2001, 73, 5358-5364.

53) F. Michopoulos, L. Lai, H. Gika, G. Theodoridis and I. Wilson, *Journal of Proteome Research*, 2009, 8, 2114–2121.

54) R. Kay, C. Barton, L. Ratcliffe, B. Matharoo-Ball, P. Brown, J. Roberts, P. Teale and C. Creaser, *Rapid Commun. Mass Spectrom.*, 2008, 22, 3255–3260.

55) P. Singh, K. Joshi, D. Guin and A. A. Prabhune, *RSC Adv.*, 2013, 3, 22319.

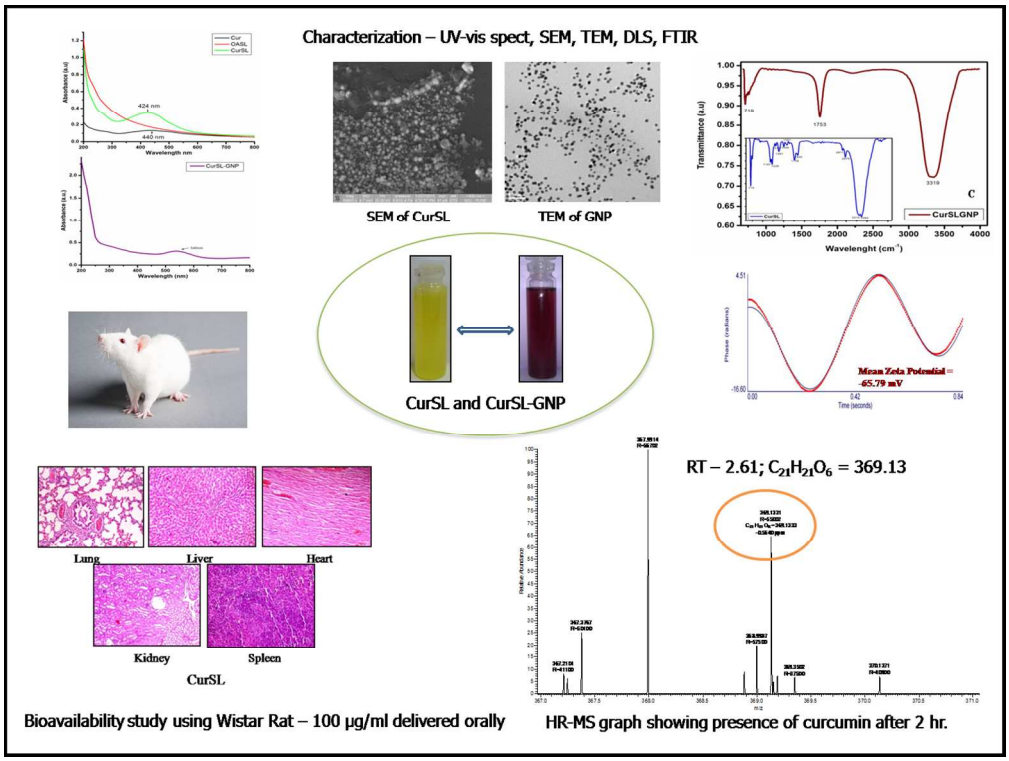

255x191mm (150 x 150 DPI)